



# Strain Measurement by Digital Image Correlation

Sen Lin, KTH – Royal Institute of Technology, Sweden

Supervisor: Ulrich Lienert, Sylvio Haas, Sven Gutschmidt

September 7, 2015

The experiments took place in former Storage Ring Doris B1

## **Abstract**

A future work for the Swedish High-Energy Materials Science beamline is the *in situ* characterization of polycrystalline samples. It requires precise sample positioning and indication of possible heterogeneities of the deformation field. Current studies show that Digital Image Correlation (DIC) is a powerful tool for both tasks. Moreover, the material for flexure joint of an essential beamline component should be selected. Therefore, a general knowledge and experience of DIC should be obtained by measuring the elastic range of candidate materials. A tensile test with DIC technique is assembled using available instrument and software. The DIC measurement is validated by strain gauge measurement and the tensile behaviors of candidate materials are characterized.

## Contents

1. Introduction .....	3
1.1 Aim of the project.....	3
2. Materials and Methods.....	3
2.1 What Is DIC .....	3
2.2 Validation of DIC Technique .....	5
2.3 Preparation of Specimens .....	6
2.4 Loading Test.....	6
2.5 Data Analysis.....	8
3. Results and Discussion .....	9
3.1 Stress-strain Curves .....	9
3.2 Modulus of Elasticity (Young's Modulus) .....	10
3.3 Deviation of the results .....	11
3.3.1 Anisotropy .....	11
3.3.2 Localization.....	12
3.4 Factors that affect the result .....	13
4. Conclusion and Future Work .....	14
Acknowledgement.....	14
References.....	15

## **1. Introduction**

The Swedish high-energy materials science beamline (P21) will operate in 2017 at DESY. The energy of the beamline is from 40 - 150 keV, which can satisfy the experiment techniques such as WAXS, SAXS, and Imaging.

A future work of the beamline is structural in situ characterization of polycrystalline bulk samples, especially materials under external stimuli. Monochromatic high-energy X-rays are focused on the sample to obtain high spatial resolution. However, metrology is required that enables precise sample positioning and also indicates possible heterogeneities of the deformation field across the samples. Digital image correlation (DIC) has been proven as a strong candidate [1] and therefore has been considered to add into the sample positioning units as a supplementary characterization method in order to map surface strains. Traditional DIC technique is difficult to meet the demand of experiment using x-ray instrument, which leads to the customization of the technique, hence, before using DIC, basic experience needs to be gained.

### **1.1 Aim of the project**

In order to learn basic knowledge about DIC, a setup is assembled based on existing devices and software. For validating of DIC, another strain measurement, strain gauge, is introduced to the testing as well. Meanwhile, the selection of material for a flexure joint of an essential beamline component (Double Laue Silicon Monochromator) should be carried out by measuring the maximum elastic deformation ranges and bulk e-moduli. A load frame and some other devices are provided for the experiment procedure design.

## **2. Materials and Methods**

### **2.1 What Is DIC**

DIC is a non-contact optical technique for measuring strains. In principle, DIC compares a series of grey-scale images of a sample at different stages of deformation, tracks pixels movement in the region of interest (ROI) [2] and calculates displacement and strain by the use of correlation algorithm.

DIC consists of at least digital camera, zoom objective and PC software. Before mechanical tests, specular markers should be applied on the sample surface in order to let the camera capture their movement and track them. Therefore, the markers are of great importance and can be obtained by spraying, etching or self-roughness (or texture). During the test, consecutive pictures are taken by one or more cameras while samples are under deformation tests, the number of cameras depends on whether the analysis is 2D or 3D and the precision one wants to achieve. Images are later transferred to PC and are analyzed through correlation algorithm by using software like Matlab and ARAMIS.

As shown in Fig. (1), images are taken by camera, before analysis, ROI was selected by user and grid will be applied over the whole ROI, then the displacement of this grid is calculated.

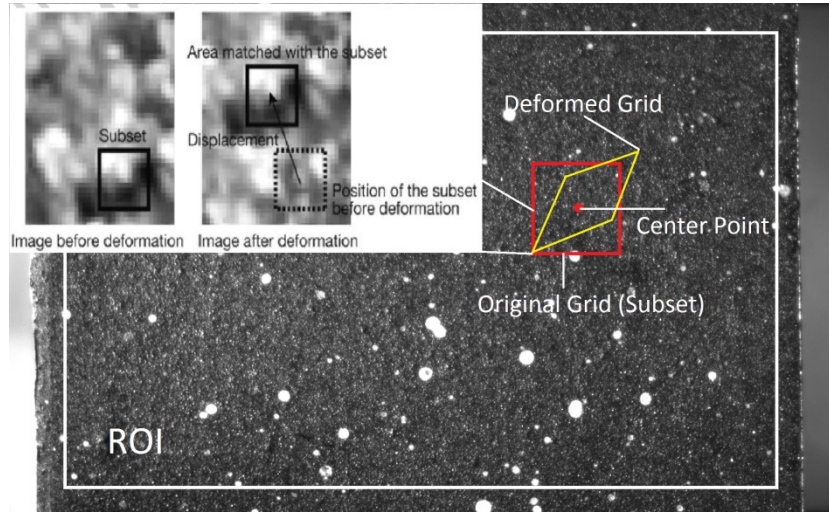


Figure 1: DIC Image with illustration of grid

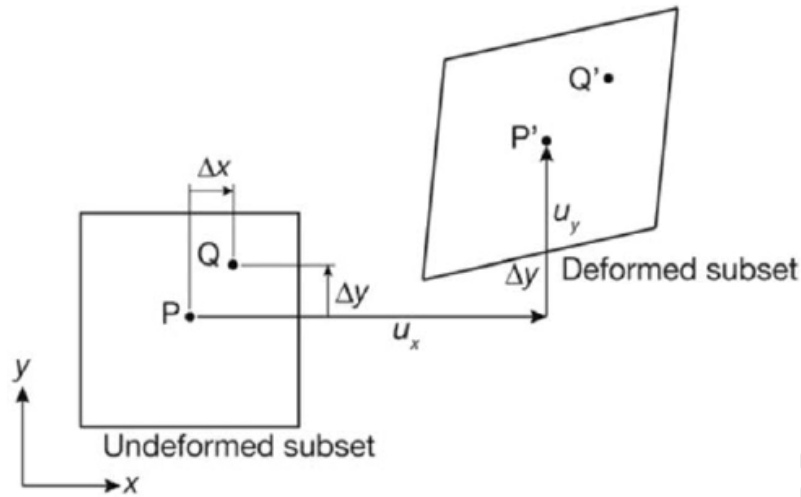


Figure 2: Subset before and after deformation

Figure (2) shows the principle of evaluation. The grid moves during the deformation, and original grid boundary will also deform to cover all the original pixels with in the grid, so coordinates for all pixels will change, for example, the center of the grid has an original coordinate of  $(x,y)$ , after deformation it changes to  $(x^*,y^*)$ , and it can be expressed as [2]:

$$x^* = x + u_x + \frac{\partial u_x}{\partial x} \Delta x + \frac{\partial u_x}{\partial y} \Delta y \quad (1)$$

$$y^* = y + u_y + \frac{\partial u_y}{\partial x} \Delta x + \frac{\partial u_y}{\partial y} \Delta y \quad (2)$$

In the Eq. (1) and (2),  $\Delta x$  and  $\Delta y$  are horizontal and vertical distance from the center of the subset to the original point  $(x,y)$ , center point P and a random point Q moved to the position of P' and Q' respectively. For the distance from P to P' is interpreted as the displacement,

and the displacement of Q is expressed by Eq. (1) and (2) and strain is obtained from the partial displacement derivatives.

From the perspective of function and economy, DIC has some outstanding advantages compare to conventional strain measurement. As a non-contact tool, DIC can obtain large visual area and provide clear image whose physical pixel size can be on the micrometer scale. This property can make DIC of great value in special testing environments such as vacuum chamber, x-ray scattering, high temperature etc. DIC has the capability to track specular patterns in subsets over the whole ROI, which means a full field measurement contains considerable amount of experimental data [3], data can be used to map the displacement contour plot and strain distribution etc. The strain maps reveal phenomena like localization, further contribute to materials studies, e.g. crystallography. Compare to other nondestructive testing, DIC possesses high economic efficiency.

## 2.2 Validation of DIC Technique

For gaining knowledge about digital image correlation it is essential to evaluate its validity by using alternative measurement at the same time. Therefore, strain gauge was implemented to the tensile tests.

Electrical conductor will change its resistance under external forces. This phenomenon is partially due to conductor's deformation and partially due to the variation of resistivity Q that caused by microstructure change, and the phenomenon is expressed by Eq. (3):

$$\frac{dR}{R_0} = \varepsilon \cdot k \quad (3)$$

Left side represents the change of electrical resistance. In the right side, strain gauge factor k is introduced to describe the behavior of resistance change [4].

Wheatstone bridge is then introduced to the measurement as it can determine the relative change in resistance. By applying a known input voltage to the bridge, the output shows the voltage change inside the circuit:

$$\frac{V_{out}}{V_{in}} = \frac{dR}{4R_0} \quad (4)$$

From above, strain can be calculated from output voltage using Eq. (3) and (4), and the general equation is:

$$\varepsilon = \frac{4V_{out}}{V_{in} \cdot k} \quad (5)$$

The accuracy of strain gauge is mainly dependent on the measuring grid, on which external environment condition such as temperature and gluing condition will affect the results.

## 2.3 Preparation of Specimens

The materials involved in loading tests are listed in table 1 [5] [6] [7].

Table 1: Materials Information

Name	Material denomination	Size (length x width x height) / mm	Additional heat treatment	Note
<b>Austenitic Stainless Steel</b>	EN 1.4301	30 x 6.95 x 0.1	/	<b>Practice Testing Material</b>
<b>Copper Beryllium</b>	AMS 4530	30 x 6.95 x 0.1	/	<b>Flexure Joint Candidate</b>
<b>Copper Beryllium (HT)</b>	AMS 4530	30 x 6.95 x 0.1	Tempered 2h at 315°C	<b>Flexure Joint Candidate</b>
<b>Beta Titanium Alloy (HT)</b>	AMS 4914	30 x 6.95 x 0.1	Tempered 8h at 540°C	<b>Flexure Joint Candidate</b>

Specimens were glued on strain gauges and placed aside for 1 hour. Then the specimens were painted with black and white color in order to obtain contrast for DIC.

## 2.4 Loading Test

The experiment setup was designed as two parts: measuring part and processing part. Figure (3) shows the main procedure of the experiment.

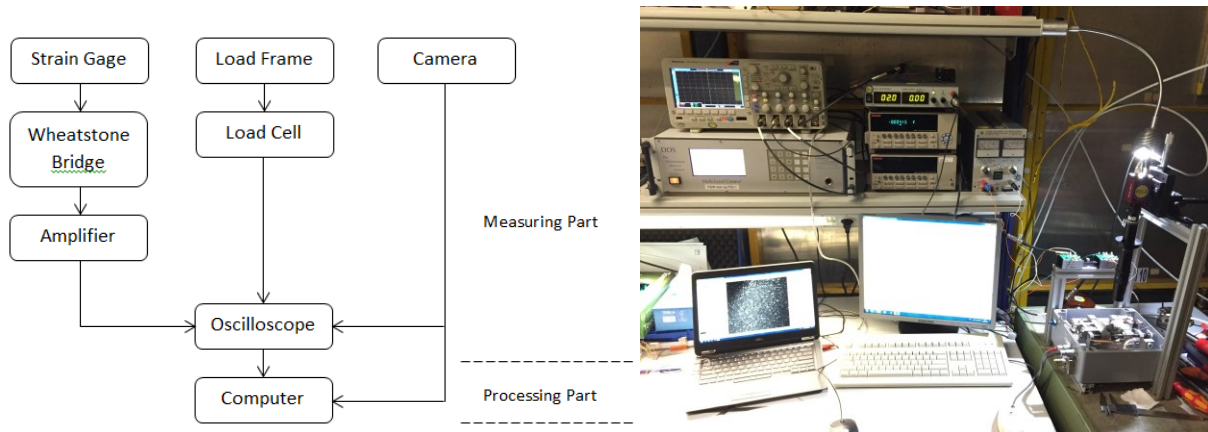


Figure 3: Experiment setup

In the strain gauge section, the voltage signal is amplified and recorded by digital oscilloscope; voltage value was real-time to avoiding accidents. The load frame was controlled by computer software DDS, the DDS controller has an analog output for recording the applied force. The CCD-camera was connected to computer in order to adjust parameters (like exposure time, zoom, acquisition frame rate, etc.) and save consecutive images. Moreover, a trigger signal was sent to oscilloscope at the moment when camera was taking pictures. After tensile tests, waveform recorded by oscilloscope was copied to computer for further analysis.

Details of instruments and software involved are listed in table 2.

**Table 2: List of instrument and software**

<b>Device &amp; Software</b>	<b>Model &amp; Version</b>	<b>Company</b>	<b>Feature</b>
Load Frame	5'000 N Tensile and Compression Module	Kammrath & Weiss GmbH	Built-in load cell with maximum tensile load 5000N
DDS	DDS 32 2.0	Kammrath & Weiss GmbH	Control the load frame
Wheatstone bridge	Bridge Completion Module BCM-1	OMEGA	Resistor Tolerance: $\pm 0.1\%$
Power Supply	ES 030-10	DELTA ELEKTRONIKA	Voltage range 0 – 30 V
Amplifier	6514 Programmable Electrometer	KEITHLEY	<1fA noise Precision up to 0.01 mV
Oscilloscope	Mixed Signal Oscilloscopes MSO 2024B	Tektronix	2 and 4 analog channels Maximum recording time 1000s 1 megapoint record length on all channels
Digital Camera	Manta G-504	Allied Vision	Resolution: 2452(h) x 2056(v)
Camera Controller	AVT Vimba Viewer 1.1.3	Allied Vision	Paired software for the camera
Matlab	Matlab R2013b 64bit & Matlab R2014b 64bit (for cluster)	MathWorks	Maximum 64 operation cores

Testing sample was connected to the Wheatstone bridge. Due to the consideration of heat generated by resistance, the excitation voltage was set to 2V; it has been proven that using this voltage, the hysteresis of strain gauge was eliminated. Later on the sample was clamped in the load frame; the free length (unclamped length) was 14mm, and the clamping force was assured by momentum wrench. After clamping, the indication on the amplifier and DDS were set to zero.

The digital camera was fixed vertically above the sample and extra illumination was added on one side of the load frame. Other parameters are listed in table 3.

During tensile test, load frame plays a critical role since it is the only source to obtain information on force, therefore it was calibrated before real tests. The control software DDS (The Deformation Devices System) can adjust the speed of deformation, it can also change the direction of the force so both loading and unloading stages can be achieved.

Table 3: Experimental Parameters

Material	Sample Code	Loading Speed	DDS resolution	CCD-camera settings	Oscilloscope Settings
Austenitic Stainless Steel	s14	2μm/s	1500N/10V	Acquisition Frame Rate: 1 image/s  Trigger Activation: Rising Edge	CH1: Strain Gauge Scale: 5.0 mV
Copper	s15	2μm/s			CH2: Elongation Scale: 1.0 V
Beryllium	s16	0.8μm/s			CH3: Load Scale: 2.0 V
Copper Beryllium (HT)	s17	1μm/s			CH4: Trigger signal Scale: 2.0 V
Beta Titanium Alloy (HT)					

During tensile test, load frame plays a critical role since it is the only source to obtain information on force, therefore it was calibrated before real tests. The control software DDS (The Deformation Devices System) can adjust the speed of deformation, it can also change the direction of the force so both loading and unloading stages can be achieved.

However, the elastic properties of the samples are unknown, and as an approximation, the loading tests were limited within a specific strain range calculated from the literature value:

$$\varepsilon_{0.2\%} = 0.2\% + \frac{\sigma_{0.2\%}}{E} \quad (6)$$

$$\varepsilon_{max} = 0.5\% + \varepsilon_{0.2\%} \quad (7)$$

$$V_{out_{max}} = \frac{k \cdot V_{in} \cdot \varepsilon_{max}}{4} = \frac{2.11 \times 2000 mV \cdot \varepsilon_{max}}{4} = 1055 \varepsilon_{max} mV \quad (8)$$

## 2.5 Data Analysis

According to table 3, voltage can be converted to force by multiplying the resolution relationship preset in the DDS device (1500N/10V):

$$F = \frac{3000 \cdot Voltage}{10} - 1500 N \quad (9)$$

Combined with Eq. (5), the stress-strain curve of strain gage measurement can be plotted using Matlab.

DIC analysis uses Matlab software with existing code and operation manual [8]; the code contains four main GUI (Graphical User Interface): image\_setup\_GUI, correlate\_images\_GUI, compute\_data\_GUI and Visualize\_data\_GUI. In order to promote the efficiency of the analysis, super computer (cluster) was used for calculating. When analyzing, parallel calculating model is preferred for cluster, all the pictures are compared with the first image, and it has one disadvantage that for large displacement, there is larger chance that the grid cannot find dots within the search zone. If this problem occurs, serial analysis with preceding image option can be used.



For plotting stress-strain curve, it is important to obtain the accurate force value corresponding to the moment when each single picture was taken. Camera signal was differentiated and the instantaneous rising edge can thus be distinguished. Force can be found according to the indices obtained from camera signal, with the strain data, stress-strain can be plotted.

E-modulus can be obtained from the curve, so can the experimental results for 0.2% yield strength ( $\sigma_{0.2\%}$ ) and its corresponding strain ( $\epsilon_{0.2\%}$ ). The elastic range is considered to be 75% of  $\epsilon_{0.2\%}$ , which has historically been used [9].

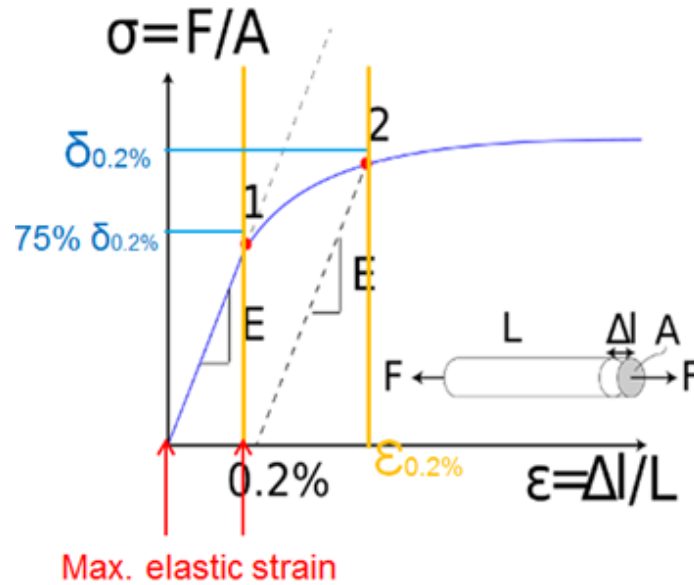
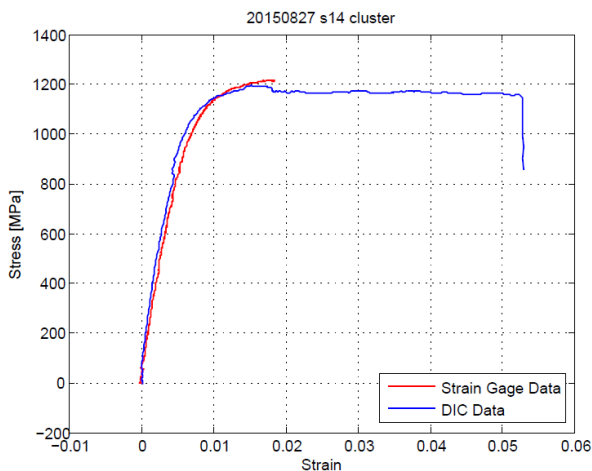


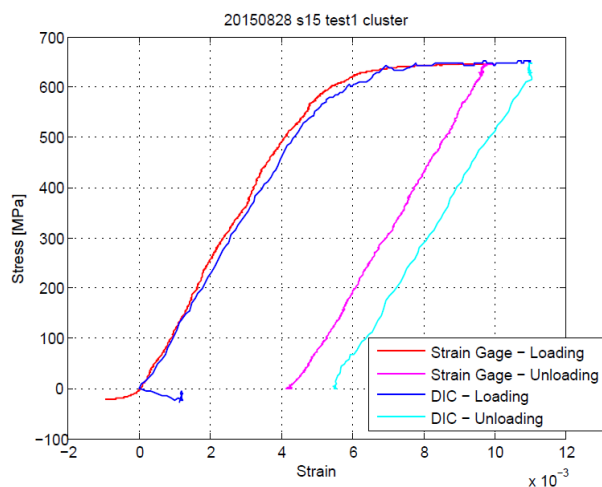
Figure 4: Principle of calculation of elastic range

### 3. Results and Discussion

#### 3.1 Stress-strain Curves



a - Austenitic Stainless Steel



b - Copper Beryllium

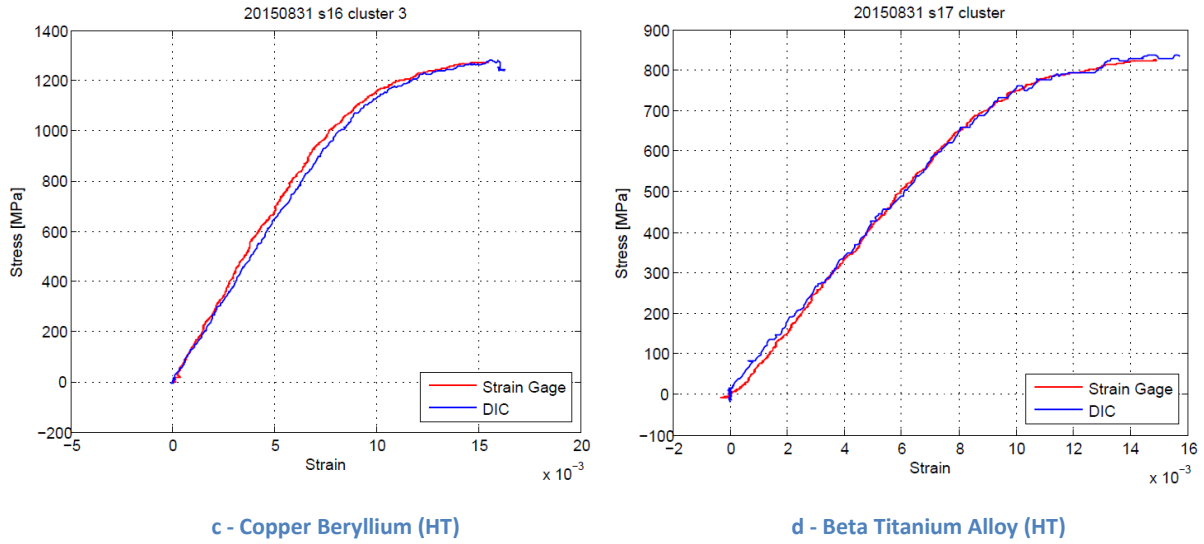


Figure 5: Stress-strain curves

Figure (6) illustrates the stress-strain curves obtained from strain gauge (red lines) and DIC measurement (blue lines). Both measurements show identical result, some variations can be caused by artifacts of DIC and other errors occurring during the experiment.

As shown in Fig. (6-a), steel sample was pulled and cracked, strain gauge measurement interrupted at the strain of approximate 1.8%. The interruption is caused by the failure of strain gauge, when the measuring grid was pulled to a certain range of strain (for LY series strain gauge is 2% strain) the grid will broke, the electrical circuit will be interrupted and amplifier value will dramatically increase. However, DIC measurement has the capability to cover the whole range of deformation therefore the complete stress-strain curve can be obtained. The sudden drop of blue line indicates that the sample fails at 5.3% strain.

Figure (6-b) shows the tensile test and later unloading process of copper beryllium without heat treatment. Two lines bifurcates below the origin, this can be explained by the clamping effect. During the clamping, forces may be applied unevenly or the sample slips, as a result sample will be bending. Before loading, the DIC tracks the specular patterns on the front side at the same time strain gauge on the reverse side yields a voltage change caused by bending. During loading, the bending sample will become flat again, DIC and strain gauge will give opposite feedbacks since one side shortens and the other side elongates. When the sample is flat, two lines get together again, and actual tensile test begins. In the unloading stage, two lines are not coincident, further investigation should be conducted to explain it.

Figure (6-c) and (6-d) show the coherence of two strain measurements.

### 3.2 Modulus of Elasticity (Young's Modulus)

E-modulus is an essential parameter describing the mechanical properties of solid materials. It can be described as the quotient of tensile stress  $\sigma$  and the strain  $\varepsilon$  in the elastic range of the stress-strain curve:

$$E = \frac{\text{tensile stress}}{\text{strain}} = \frac{\sigma}{\varepsilon} \quad (10)$$

In other words, the tangent of stress-strain curve indicates the e-modulus of the sample. Comparison between literature values and experimental results are listed below.

Table 4: Properties from literature and result

Material	E-modulus (literature) [GPa]	E- modulus from DIC [GPa]	0.2% yield strength ( $\sigma_{0.2\%}$ ) (literature) [MPa]	0.2% yield strength ( $\sigma_{0.2\%}$ ) from DIC [MPa]	Elastic Range Strength [MPa]	Elastic Range (75% $\varepsilon_{0.2\%}$ ) [%]
Steel	200	173	965	1106	827	0.46
CuBe	131	119	620-800	634	475	0.41
CuBe (HT)	131	129	1130-1420	1177	883	0.71
Beta Ti (HT)	82	80	1172	794	596	0.73

### 3.3 Deviation of the results

Deviation is a straightforward way to assess the correctness of the experiment, it can be expressed by:

$$\text{Deviation} = \frac{\text{Literature Value} - \text{Experiment Result}}{\text{Literature Value}} \times 100\% \quad (11)$$

For s14, s15, s16, s17, the deviation is 12.5%, 9.2%, 1.5% and 2.4% respectively. The difference between measured E-moduli and literature values is considered to be the result of the anisotropy of the sample or localization that has occurred in regions that were not in the visible region of DIC and strain gauge.

It is obviously that for CuBe (HT), the yield strength is almost doubled compare to CuBe without heat treatment. During heat treatment process, beryllium rich particles form in the based matrix, which is so called age hardening (precipitation hardening).

#### 3.3.1 Anisotropy

Anisotropy is a material's directional dependence of a physical property, e.g. E-modulus can vary with the loading direction. In cubic materials, the elastic moduli can be different along any crystal orientation. For polycrystalline materials, elastic properties can be described as the sum of all single crystals' properties, for instance orientation, the relationship with neighbor and microstructure [10]. Macroscopic anisotropy can occurs during cold forming, especially for foil, it has been deformed at large extent, and the microstructure can have a strong preferred orientation that leads to different complexities of deformation.

### 3.3.2 Localization

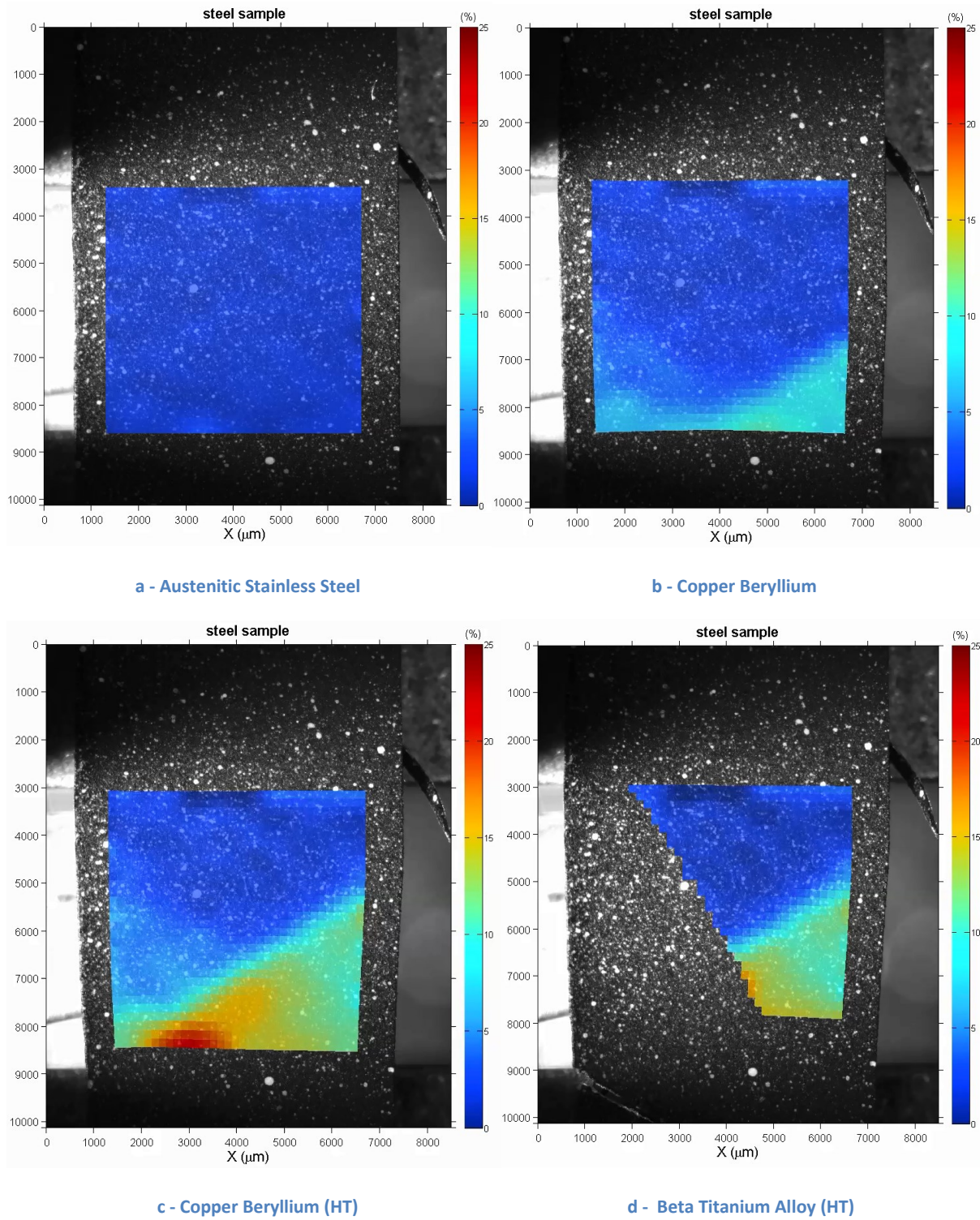


Figure 6: Strain contour plots

Figure (7) shows the deformation of austenitic stainless steel. First the sample deformed homogeneously, the strain is even over the ROI (Fig. (7-a)). As the pulling continues, the lower part of the sample has more plastic deformation, and necking forms, as it can be seen in Fig. 7-b. The cross section of necking region has less area compared to other part of the sample, stress concentration due to some internal defects such as poles and impurities (Fig.

(7-c)), and the stress thus became higher, which gives more serious impact and leads to crack (Fig. (7-d)).

This phenomenon is called localization. Localization usually happens in the materials with negligible. In principle, deformation begins in the grain whose slip system is of the same direction of the external forces. Dislocations in the grain will move to the grain boundary and later on other grains start to deform.

### **3.4 Factors that affect the result**

The measuring material of strain gauge, the leading wire and also the sample material will change their properties to temperature change. Also the bonding between gauge (most importantly the measuring grid part) and sample surface must not have any pores.

In load frame, the friction between the load cell and the yoke will yield abnormal stress-strain curve, that lubrication of the load cell is an important process. Clamping is also important, if strain gauge, glue layer or the DIC print layer is clamped, there will be a gap between the clamp and sample, during the tensile testing, and it may cause slip of the sample.

For DIC measurement, sufficient illumination is a critical factor for obtaining high quality images, the analysis will benefit from the light to a large extent, and the light direction should also be vertical to the sample surface, otherwise shades result from irregularity of the surface will change and therefore affect the correctness of analysis. Fine and even speckle pattern will also benefit the analysis.

On the other hand, parameters and software setup that involved plays a main role in the analysis, by adjusting which the result will be closer to the actual value. During analysis, the step size is of importance to the accuracy of the result, step size defines a calculation grid, in which the specular pattern is tracked and the distance from dots to the center of each grid is calculated. So in principle, the finer the grid is the better result we can get. However, sizes of the dots will affect the tracking procedure, if the size is larger than the subset size, when there is a big displacement, the grid cannot find the dots within this search zone and thus lose the displacement information. Therefore, fine grid with large search zone and small subset size can yield great result, however, it will take days to finish one analysis, and the software setup is considered according to time consumption.

Compute\_data\_GUI can smooth the data for better result; default setting for smoothing was used. For strain algorithm, in general cubic (16-node) can obtain better result for analysis with few images, otherwise linear (4-node) is preferred with large amount images analysis and it saves time.

Since the width of the sample is small, one should make sure the sample is placed parallel to the direction of external force, if the sample tilts, shear stress will appear and influence the process.

## **4. Conclusion and Future Work**

Digital Image Correlation becomes more popular these years because of its powerful function such as strain and displacement mapping and cost efficiency. DIC can also connect the experiment with numerical modeling, which can be used in many studies and simulations.

From this experiment, basic DIC technique is studied, knowledge about general procedure and factors that affect analysis result are well known. With the validation by strain gauge measurement, DIC has proven to be an accurate technique for most cases involved in the project. For testing four samples' tensile properties, DIC measurement has simpler preparing process than strain gauge measurement, and it shows reasonable results.

According to table 4, among all candidates, heat treated copper beryllium shows large elastic range and relatively high E-modulus, therefore it is selected to be the suitable material for bending hinge. The copper beryllium sheets from which the samples were cut are rather flat as compared to the titanium sheets which favor the use of copper beryllium for the flexure hinge.

In this project, 2D DIC shows its capability to handle the thin sample tensile test. However, besides experimental condition can be perfected, more details can be investigated by supplementary and novel methodologies. For example, SEM-DIC is an advanced mean for study nano- and micro-scale phenomena, together with EBSD, microstructure can also be linked to the deformation behavior [11], thus further study such as anisotropy and localization can be achieved.

## **Acknowledgement**

I would like to thank my supervisors: Ulrich Lienert, Sylvio Haas, Sven Gutschmidt for guiding use through the whole period of summer student. For Sven he taught us a lot about how to set up the experiment and prepare the samples, also he showed us how an engineer works, which is also valuable for expanding my horizons; for Sylvio, he taught us a lot about how to use software like Matlab, and helped us with the report and presentation; for Ulrich, he gave us the chance to come to work here and supervised us in the overall direction. Also I want to thank my colleague Pang Kit Jerry Lam for working with me and helping me and DESY for organizing such wonderful program.

It was a great pleasure working in DESY and I learned and experienced a lot from people i meat here.

## References

- [1] J. Kang, "Microscopic Strain Mapping Based on Digital Image Correlation," in *Proceedings of the XIth International Congress and Exposition*, Orlando, 2008.
- [2] N. McCormick and J. D. Lord, "Digital Image Correlation," *Materials Today*, vol. 13, no. 12, pp. 52-54, December 2012.
- [3] S. Roux, J. Réthoré and F. Hild, "Digital Image Correlation and Fracture: An Advanced Technique for Estimating Stress," *Journal of Physics D: Applied Physics*, vol. 42, no. 21, p. 214004, 21 October 2009.
- [4] K. Hoffmann, *An Introduction to Measurements using Strain Gages*, Darmstadt: Hottinger Baldwin Messtechnik GmbH, 1989.
- [5] Outokumpu, "EN 1.4301, AISI 304 EN 1.4307, AISI 304L," April 2009. [Online]. Available: [http://www.outokumpu.com/SiteCollectionDocuments/Austenitic-Stainless-Steel-1.4304-1.4307\\_Datasheet.pdf](http://www.outokumpu.com/SiteCollectionDocuments/Austenitic-Stainless-Steel-1.4304-1.4307_Datasheet.pdf). [Accessed 06 September 2015].
- [6] M. B. P. Alloys, "Alloy 25 (C17200) Strip," 2013. [Online]. Available: <http://materion.com/~media/Files/PDFs/Alloy/DataSheets/CopperBeryllium/AD0068-0311%20Alloy%2025%20Strip.pdf>. [Accessed 06 September 2015].
- [7] I. Ulbrich Stainless Steels & Special Metals, "TI 15-3-3-3, (15-333), UNS R58153 Strip, Coil, Foil & Wire, AMS 4914," 2015. [Online]. Available: [http://www.ulbrich.com/wp-content/uploads/2015/06/Ti-15-3-3-3\\_Ulbrich-Revision-06.01.2015.pdf](http://www.ulbrich.com/wp-content/uploads/2015/06/Ti-15-3-3-3_Ulbrich-Revision-06.01.2015.pdf). [Accessed 06 September 2015].
- [8] E. M. Jones, "Documentation for Matlab-based DIC code," University of Illinois at Urbana-Champaign, 2015.
- [9] M. B. P. Alloys, "Yield Strength and Other Near-Elastic Properties," November 2012. [Online]. Available: <http://materion.com/~media/Files/PDFs/Alloy/Newsletters/Technical%20Tidbits/Issue%20No%2047%20-%20Yield%20Strength%20and%20Other%20Near-Elastic%20Properties.pdf>. [Accessed 06 September 2015].
- [10] U. F. Kocks, C. N. Tomé and H. -R. Wenk, *Texture and Anisotropy Preferred Orientations in Polycrystals and their Effect on Materials Properties*, Cambridge: Cambridge University Press, 2000.
- [11] A.D. Kammers and S. Daly, "Digital Image Correlation under Scanning Electron Microscopy: Methodology and Validation," *Experimental Mechanics*, vol. 53, no. 9, pp. 1743-1761, 2013.